

THE ANOMALOUS INFRARED EMISSION OF ABELL 58

Josef Koller¹

*Department of Physics & Astronomy, MS-108, Rice University, Houston, TX 77005
Theoretical Astrophysics, T-6, MS B288, Los Alamos National Laboratory, NM 87545*

and

Stefan Kimeswenger²

Institute of Astrophysics, University of Innsbruck, A-6020 Innsbruck, Austria

ABSTRACT

We present a new model to explain the excess in mid and near infrared emission of the central, hydrogen poor dust knot in the planetary nebula (PN) Abell 58. Current models disagree with ISO measurement because they apply an average grain size and equilibrium conditions only. We investigate grain size distributions and temperature fluctuations affecting infrared emission using a new radiative transfer code and discuss in detail the conditions requiring an extension of the classical description. The peculiar infrared emission of V605 Aql, the central dust knot in Abell 58, has been modeled with our code. V605 Aql is of special interest as it is one of only three stars ever observed to move from the evolutionary track of a central PN star back to the post-AGB state.

Subject headings: ISM: dust, planetary nebulae: individual (V605 AQL), stars: circumstellar matter, methods: numerical

1. INTRODUCTION

The first evidence of a significant discrepancy between measurements and predictions of standard models for infrared (IR) emission from dust was noticed by Andriesse (1978). He found that IR emission of the H II region M17 and the diffuse galactic emission is at 11 μm

¹Email: josef@rice.edu

²Email: stefan.kimeswenger@uibk.ac.at

and $20\ \mu\text{m}$ considerably higher than standard predictions (Mathis, Mezger, & Panagia 1983; Puget & Leger 1989). Andriesse (1978) pointed out that spatial temperature variations cannot solve the conflict between model predictions and measurements, but temperature fluctuations of the dust grains themselves could. In general, small dust particles have a lower heat capacity due to their smaller size. Therefore, particles with radii smaller than $20\ \text{\AA}$ to $50\ \text{\AA}$ follow temperature fluctuations, but this range strongly depends on the radiation field. Moreover, if the grain has time to cool down, i.e. no continuous photon impact and heating, the emitted IR photons of a sample of dust grains have a spectral energy distribution (SED) which differs from that in the equilibrium case. The temperature of such grains can be modeled by means of a temperature distribution function $P_a(T)$. Various groups have studied temperature fluctuations of small grains and proposed numerical methods for the calculation (Gail & Sedlmayr 1975; Purcell 1976; Draine & Anderson 1985; Desert, Boulanger, & Shore 1986; Dwek 1986). However, a more powerful technique was introduced by Guhathakurta & Draine (1989) to find the temperature distribution and the associated infrared emission. This method can be easily implemented into a computer code and is reasonably fast. A further description of the technique can be found in Borkowski et al. (1994); Siebenmorgen, Kruegel, & Mathis (1992), and an advanced extension of the method was published by Manske & Henning (1998).

We discuss the emission of real grain size distributions for thermal equilibrium and non-equilibrium conditions in the following section. We applied our new radiative transfer code to the central dust knot V605 Aql in Abell 58 (a result of a late-helium flash in 1919). A proper model of the current state of the circumstellar shell, completely shielding the new central star, is important to understand the physical process of dust formation and of the mass ejection history. This object illustrates stellar evolution in real time. Our model of the circumstellar shell around the central star does not only use the dust component, rather it combines gas and dust to obtain a more accurate description of V605 Aql.

2. THERMAL EQUILIBRIUM AND NON-EQUILIBRIUM

Temperature is one of the most important physical parameters of a dust grain. In this work only heating by photons is considered. The calculation of the temperature of a dust grain is, under the assumption of thermal equilibrium conditions, usually straight-forward, i.e., the energy absorbed from the ambient radiation field is precisely matched by the energy

emitted, and thus an equilibrium temperature is attained:

$$c \int_0^{\infty} u_{\lambda} Q_{abs}(a, \lambda) d\lambda = 4\pi \int_0^{\infty} Q_{abs}(a, \lambda) B_{\lambda}(T_d) d\lambda \quad (1)$$

where u_{λ} is the density of the heating radiation field. $Q_{abs}(a, \lambda)$ are the efficiency factors for absorption for a dust grain with radius a at different wavelengths λ , and $B_{\lambda}(T_d)$ is the blackbody emission of a grain at temperature T_d . In the case of thermal equilibrium it is sufficient to solve the equation above, but a size distribution of dust grains has to be included.

Laboratory experiments and theoretical considerations suggest that the mass distribution of dust particles is described as

$$n(m)dm \propto m^{-p}dm \quad (2)$$

where p is a constant and $n(m)$ is the number of grains in the range from m to $m + dm$. Mathis, Rumpl, & Nordsieck (1977), hereafter MRN, applied this relation to extinction measurements of the interstellar medium and found a power law of $p = 3.5$ for the general interstellar medium (ISM). Infrared objects have a much higher excess in mid-infrared and near-infrared (MN-IR) than simple dust models predict, but applying a grain size distribution can lead to a better agreement between measurements and models. However, if the dusty material is situated in a dilute radiation field, then the assumption of thermal equilibrium is not valid. The dust temperature changes due to the stochastic process of grain heating and has to be treated in a more sophisticated way as described below.

Considering a spherical dust particle of radius a and with a heat capacity per unit volume $C(T_d)$, the internal energy of a dust particle is calculated using

$$U(a, T_d) = \frac{4\pi a^3}{3} \int_0^{T_d} C(T') dT'. \quad (3)$$

If an incident photon deposits the energy E on the dust particle, the energy will be distributed almost instantly and will raise the temperature of the grain by an amount of δT_d according to $E = U(a, T_d + \delta T_d) - U(a, T_d)$. If the dust grain is sufficiently small and thus $E \gg U(a, T_d)$, the dust particle will experience a strong rise in temperature. For larger dust grains or high photon densities, the energy provided by a single photon is negligible compared to the internal energy of the grain. In this case the dust grain will fluctuate with a small amount around the equilibrium temperature, i.e., the temperature distribution function of the dust grain is approximately a small Gaussian centered on T_d which can be written as a delta distribution for very small fluctuations.

Temperature fluctuations have to be taken into account, if: (1) The density of the radiation field is low, (2) the radiation field contains high-energy photons providing the grain with a large amount of energy compared to the internal energy, (3) the grain size is small ($a < 100 \text{ \AA}$) and, therefore, internal energy is low. These circumstances are obviously met for small grains in the ISM or for PNe, because the radiation field is weak but contains many high-energy photons.

3. THE HYDROGEN–POOR KNOT V605 AQL

3.1. Introduction to V605 Aql

Some central stars of planetary nebulae (PNe) experience a final thermal pulse (Iben et al. 1983) after starting the descent along the cooling track towards white dwarfs. Theoretical calculations show that during such a pulse the remaining hydrogen is completely incorporated into the helium-burning shell. The object then briefly expands to the dimension of an AGB star and proceeds with helium burning. It follows nearly the same path in the Hertzsprung-Russell diagram (HRD) as during the hydrogen burning when the initial excitation of the nebula occurred. The evolution is very fast, and Iben et al. (1983) suggested that it would be too short to be observable. However, at least three stars have been found during their rapid brightening caused by a final helium flash. (1) Sakurai’s Object or V4334 Sgr was caught during a nova-like outburst in 1996. (2) FG Sagittae brightened in the year 1894. (3) V605 Aql was discovered in 1919 and was mistaken to be a slow nova. Since these objects evolve very quickly, especially Sakurai’s object, on time-scales from weeks to years, they provide the rare opportunity for studying stellar evolution in real time.

The evolution of the late helium flash object V605 Aql (IRAS 19158+0141) is reviewed in the paper by Clayton & de Marco (1997). Starting in August 1919 the object brightened within two years from $m_{pg} \approx 15^m$ to $m_{pg} \approx 10^m$. Its peculiarity was noted in a spectrum in 1921, but after a few phases of fading and brightening it got too weak, and therefore nothing can be found in the literature until 1971 (Ford 1971). At that time V605 Aql was recognized as a star/nebulosity (diameter $\sim 1''$) in the geometric center of the PN Abell 58 (Abell 1966), which has a size of $44'' \times 36''$. The spectrum of the outer nebula Abell 58 is typical for a PN. However, it has a weaker H_α than [N II] emission. Seitter (1987) took a spectrum of the central knot V605 Aql after Pottasch et al. (1986) suggested that it is a hydrogen poor object. Seitter derived physical conditions for the inner and outer nebula from the lines [O III] (4959 \AA , 5007 \AA) along with [N II] (6548 \AA , 6584 \AA) and [O I] (6300 \AA , 6363 \AA). However, these values are quite uncertain and yield contradictory results from different spectra due to high noise. The abundance of elements can only be estimated

because of the weakness of diagnostic lines. Recent determinations for both, Abell 58 and V605 Aql are made by Guerrero & Manchado (1996).

Seitter (1987) found in her spectra that V605 Aql shows a C IV feature (5800 Å), which suggests that the central star is of Wolf-Rayet [WC] type, but it was not possible to clearly differentiate this feature from non-stellar lines. However, in Guerrero & Manchado (1996) it is clearly identified. The correction for dust absorption is "merely a guesswork" (Seitter 1987). With $T = 100,000$ K and $A_V = 4^m$ at a distance of 3.5 kpc, the obtained luminosity is $300 L_\odot$ but this would place the object in the HRD at a position which is reached 1000 years after the late helium flash for a $0.5 M_\odot$ star. Compared to the reported nova event in 1919 this would be one order of magnitude too large. Moreover, the integration over the infrared spectrum at 3.5 kpc leads to a luminosity of about $2500 L_\odot$, which is still too low to account for the recent event. Therefore, we adopt a distance of 5 kpc to place V605 Aql at a proper position ($5800 L_\odot$) in the HRD.

Seitter (1987) reports a radial expansion velocity of the inner knot of 60 km s^{-1} . In contrast, Pollacco et al. (1992) find with high resolution and high S/N spectra a value of about 100 km s^{-1} . The outflow of the central knot in Abell 58 is completely hydrogen depleted, and the ISO spectra taken by Harrington et al. (1998) show no PAH feature, as is expected for a H-poor carbon rich outflow.

Observations with ISOCAM yield a bright MN-IR emission from the central knot in Abell 58. Kimeswenger, Kerber, & Weinberger (1998) concluded that a simple dust emission model cannot explain the SED. The ISO observations, which we use here (Table 1), are recalibrated with ISO data reduction software OLP V.5 (Siebenmorgen & Blommaert 1999). Note that the extreme 1 to 3 μm excess reported in Kimeswenger, Kerber, & Weinberger (1998) is caused by a misidentification in the NIR photometry in the past (see Kimeswenger, Koller, & Schmeja 2000 for further details).

3.2. The Model for V605 Aql

We linked our numerical code NILFISC (Near Infrared Light From Interstellar Scattering Code) to the photoionization code CLOUDY (Ferland et al. 1998) to combine gas and dust models. This was implied by using small shells of gas (CLOUDY) and dust (NILFISC) providing each other with the input radiation (Fig. 1). CLOUDY calculates the gas continuum and emission lines of the first shell and serves the radiation as an input for NILFISC. NILFISC then adds extinction and dust emission to this shell and provides the radiation for the next gas shell calculated again by CLOUDY and so forth. The number of sub-shells

required for this calculation technique were extensively tested to (a) optimize the CPU time and (b) to minimize numerical difficulties. We describe numerical and stability tests for various types of sources in Koller (1999); Koller & Kimeswenger (2001). A more extensive and detailed version can be found in Koller (2000) which is obtainable as a postscript version from the authors upon request.

The dust shell model in V605 Aql utilizes a decreasing dust density $\propto 1/r^2$, which is consistent with the model of a steady outflow at a constant velocity during a short nucleation period (Rowan-Robinson & Harris 1983). The outflow is carbonaceous and contains no silicate or PAH signatures (Harrington et al. 1998). Therefore, we applied the optical properties of carbon grains (Laor & Draine 1993) to model this object. The value of $A_V = 7^m$ is in the range of preceding extinction evaluations. We chose A_V according to the literature and configured our dust shell density for this value finding a gas to dust ratio of 10/1 in an almost H-less outflow. On the basis of the youth of the object, a filling factor near unity can be assumed as has been already successfully applied to other very young optical thick shells (Siebenmorgen, Zijlstra, & Kruegel 1994). We used a blackbody central star with a temperature of 100,000 K and a luminosity $5800 L_\odot$ as the heating source for the dust shell. These values are supported by evolutionary track models. At a smaller distance the required luminosity would be too low compared to theoretical predictions (Bloeker 1995b). At a larger distance the old PN, Abell 58, would become too large compared to its surface brightness. By fixing the distance to 5 kpc, a lower boundary for the total luminosity can be found by integration of the SED defined by the ISOCAM and IRAS measurements.

The inner radius and the grain size distribution inside the dust shell are left as free parameters. However, the power law of the grain size distribution is assumed to be constant throughout the rather small shell (5×10^{13} m). A limit of the outer radius can be set to a maximum of $2''$ (Geckeler, Kimeswenger, & Koller 1999). This is also in agreement with optical measurements by Guerrero & Manchado (1996). The parameters for the shell size are supported by velocity determinations by Pollacco et al. (1992) providing $v_{\text{exp}} \approx 100 \text{ km s}^{-1}$ for the inner knot. However, the line profile wings have not been taken into account, and according to Schönberner & Steffen (1999) such expansion estimations are too low by 20-30%, yielding $v_{\text{exp}} \approx 120 \text{ km s}^{-1}$. Assuming a constant v_{exp} , this value leads to a shell radius of 2.6×10^{14} m after 70 years, which was the age of the object at the time of measurements by Pollacco et al. (1992). The dust shell size, the total extinction, and the assumed density profile provide us with the total dust mass.

The H-poor nature of V605 Aql was taken into account by using a virtually H-less gas mixture in CLOUDY. We chose H/He $\approx 10^{-6}$ below the solar value to simulate the H under-abundance (other elements in respect to He). This approach removes the 912 Å

absorption edge of hydrogen, and the He ionization at 54 eV becomes dominant for the gas absorption. This leaves more UV photons to be absorbed by small dust particles, which have major absorption efficiencies at 750 Å and 2200 Å (famous extinction interstellar extinction bump). Usually the first feature is not very efficient because hydrogen Lyman absorption between 13 eV and 54 eV has already removed most of the absorbable photons.

4. RESULTS

Figure 2 shows the emission of a pure dust shell for various distances from the central star. Both methods, with temperature fluctuations and equilibrium temperatures, were used to investigate at which distance they start to differ. In the case of such a high luminosity object ($L_* \sim 6000 L_\odot$, $T \sim 100,000$ K) and with dust grains at a distance of 10^{13} m, temperature fluctuation generally do not arise. If the grains are at a distance of 10^{14} m, the two methods start to show a discrepancy at $\lambda \lesssim 3 \mu\text{m}$. For grains at larger distances to the central star the discrepancy rises quickly up to larger wavelengths. For grains at 0.3 pc (10^{16} m) the two methods differ already for wavelengths $\lambda \lesssim 11 \mu\text{m}$. Note that this is only true for a grain size distribution.

We derived a dust shell radius of $2.5 - 3.0 \times 10^{14}$ m for V605 Aql, which means that we are dealing with a "borderline" object where temperature fluctuations start to get important (Figure 2), although the ionization edges of the gas and internal extinction of the object further dilutes the UV radiation field. We conclude that V605 Aql is actually on the lower boundary where temperature fluctuations have to be considered. In V605 Aql the emission by temperature fluctuations may be approximated in first order by applying the method of equilibrium temperature computations, but a single grain size model is not a proper approximation (see Figure 3). This Figure also shows the gas emission taking over at wavelengths about $1 \mu\text{m}$. The strong but narrow emission lines, visible in the model, do not significantly contribute to the wide band flux. Table 2 provides the parameters we used for our model.

In Figure 4 we compare two different models (with and without temperature fluctuations). V605 Aql is affected mainly in the wavelength range of $2 \mu\text{m} \leq \lambda \leq 5 \mu\text{m}$. This is on one hand due to the fact that the shell radius is rather small and on the other hand, the hydrogen, usually depleting the UV radiation below 91.2 nm, is strongly under-abundant.

Compared to the dust mass predicted by evolutionary model computations (Bloecker 1995a), the dust mass in our model is rather high. However, the model assumes a spherically symmetric dust shell requiring a copious amount of dust. Pollacco et al. (1992) did not

exclude that the ejection could be in the form of a symmetric shell. It could also be a bipolar outflow of which we only see the blue shifted side, as also indicated in Guerrero & Manchado (1996). Non-spherical shell models are planned to reduce this discrepancy. The current version, although now applying spherical symmetry, was written highly modular. Using small plane parallel slabs, will allow us to extend the code to 2D and 3D geometry in nearby future.

5. CONCLUSION

The IR emission caused by the hot components of dust grains undergoing temperature fluctuations due to single-photon heating events is observed in a variety of regions: in the interstellar medium, in H II regions, reflection nebulae, planetary nebulae, interstellar medium, cirrus, and at the edges of dense molecular clouds. The dependence of the distribution of this emission upon the spectral energy distribution shows that UV photons from very hot stars dominate this mechanism.

The results from the code NILFISC, developed for the calculations presented here, show that introducing a real grain size distribution improves the situation significantly and that a equilibrium temperature model with a single average grain size is not sufficient. However, the use of the temperature fluctuation technique for small dust grains is not necessary in dense radiation fields and much computing time can be saved if the sophisticated method with stochastic heating is not required. Our code evaluates the situation for every grain size individually.

The model of the born-again core V605 Aql of the PN Abell 58 is able to describe the ISO and IRAS observations. Although the dust shell is small and the heating source very luminous, the application of a grain size distribution but only with equilibrium calculations yield in a discrepancy of about 40 percent at short IR wavelengths. V605 Aql is a borderline case: at lower radii, higher luminosities, or a cooler illuminating source, temperature fluctuations do not have to be taken into account.

In contrary to previous work (Seitter 1987; Guerrero & Manchado 1996; Clayton & de Marco 1997), we had to adopt a larger distance (5 kpc) and a higher luminosity ($5800 L_{\odot}$) for a satisfactory fit of our model to observations. The higher luminosity is in much better agreement to evolutionary models (Bloeker 1995a,b) than the derived luminosity of e.g. $300 L_{\odot}$ in Seitter (1987). To keep consistency with the observed flux, the higher luminosity requires a larger distance (5 kpc) than the usually cited value of 3.5 kpc (Clayton & de Marco 1997).

Because most planetary nebulae are larger and have hot central stars, the technique with temperature fluctuations ought to be applied to most of them.

This work has been supported by the Austrian *Fond zur Förderung der wissenschaftlichen Forschung*, project number P11675-AST. We would like to thank P. Hartigan and the referee for valuable suggestions and comments.

REFERENCES

- Abell, G. O. 1966, ApJ, 144, 259
- Andriessse, C. D. 1978, A&A, 66, 169
- Bloecker, T. 1995, A&A, 297, 727
- Bloecker, T. 1995, A&A, 299, 755
- Borkowski, K. J., Harrington, J. P., Blair, W. P., & Bregman, J. D. 1994, ApJ, 435, 722
- Clayton, G. C. & de Marco, O. 1997, AJ, 114, 2679
- Draine, B. T. & Anderson, N. 1985, ApJ, 292, 494
- Desert, F. X., Boulanger, F., & Shore, S. N. 1986, A&A, 160, 295
- Dwek, E. 1986, ApJ, 302, 363
- Ferland, G. J., Korista, K. T., Verner, D. A., Ferguson, J. W., Kingdon, J. B., & Verner, E. M. 1998, PASP, 110, 761
- Ford, H. C. 1971, ApJ, 170, 547
- Gail, H. & Sedlmayr, E. 1975, A&A, 43, 17
- Geckeler, R. D., Kimeswenger, S., & Koller, J. 1999, Proceedings of 2nd Austrian ISO Conference, Vienna May 1999, eds. Hron, J.; Hoefner, S., 105
- Guerrero, M. A. & Manchado, A. 1996, ApJ, 472, 711
- Guhathakurta, P. & Draine, B. T. 1989, ApJ, 345, 230
- Harrington, J. P., Lame, N. J., Borkowski, K. J., Bregman, J. D., & Tsvetanov, Z. I. 1998, ApJ, 501, L123

- Iben, I., Kaler, J. B., Truran, J. W., & Renzini, A. 1983, *ApJ*, 264, 605
- Kimeswenger, S., Kerber, F., & Weinberger, R. 1998, *MNRAS*, 296, 614
- Kimeswenger, S., Koller, J., & Schmeja, S. 2000, *A&A*, 360, 699
- Koller, J. 1999, *ASP Conf. Ser.* 188: *Optical and Infrared Spectroscopy of Circumstellar Matter*, 271
- Koller, J. 2000, MSc thesis, University Innsbruck, Austria
- Koller, J. & Kimeswenger, S. 2000, *ASP Conf. Ser.* 196: *Thermal Emission Spectroscopy and Analysis of Dust, Disks, and Regoliths*, 23
- Koller, J. & Kimeswenger, S. 2001, *Ap&SS*, 275, 121
- Laor, A. & Draine, B. T. 1993, *ApJ*, 402, 441
- Manske, V. & Henning, T. 1998, *A&A*, 337, 85
- Mathis, J. S., Mezger, P. G., & Panagia, N. 1983, *A&A*, 128, 212
- Mathis, J. S., Rumpl, W., & Nordsieck, K. H. 1977, *ApJ*, 217, 425
- Pollacco, D. L., Lawson, W. A., Clegg, R. E. S., & Hill, P. W. 1992, *MNRAS*, 257, 33P
- Pottasch, S. R., Mampaso, A., Manchado, A., & Menzies, J. 1986, *IAU Colloq. 87: Hydrogen Deficient Stars and Related Objects*, 359
- Puget, J. L. & Leger, A. 1989, *ARA&A*, 27, 161
- Purcell, E. M. 1976, *ApJ*, 206, 685
- Rowan-Robinson, M. & Harris, S. 1983, *MNRAS*, 202, 767
- Schönberner, D. & Steffen, M. 1999, *ASP Conf. Ser.* 188: *Optical and Infrared Spectroscopy of Circumstellar Matter*, 281
- Seitter, W. C. 1987, *The Messenger*, 50, 14
- Siebenmorgen, R., Kruegel, E., & Mathis, J. S. 1992, *A&A*, 266, 501
- Siebenmorgen, R., Zijlstra, A. A., & Krugel, E. 1994, *MNRAS*, 271, 449
- Siebenmorgen, R. & Blommaert J. 1999, *ISO Handbook Volume III (CAM)*, Version 1.0, ISO Science Data Centre, Astrophysics Division of ESA

van der Veen, W. E. C. J., Habing, H. J., & Geballe, T. R. 1989, *A&A*, 226, 108

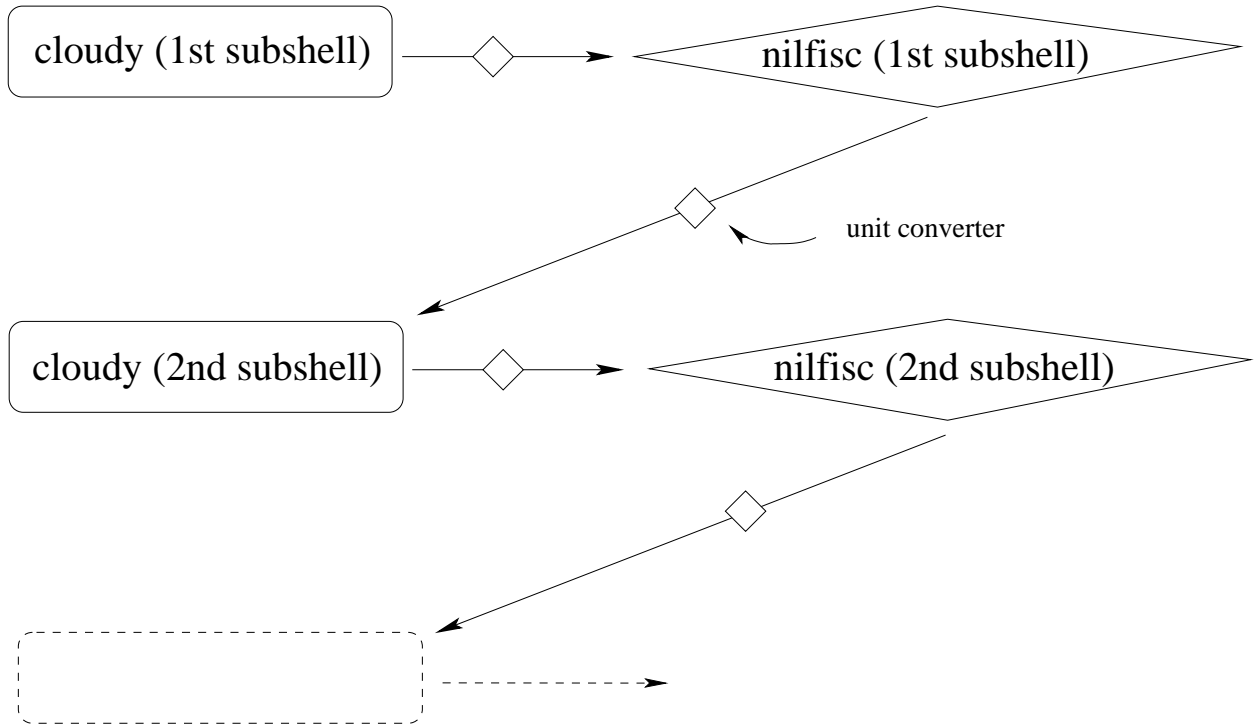


Fig. 1.— Scheme for the calculation sequence. The first subshell of gas is computed with CLOUDY which serves the output radiation to NILFISC. NILFISC calculates the extinction and emission from the dusty component and delivers the total output radiation of the first subshell (gas and dust) to CLOUDY and so forth.

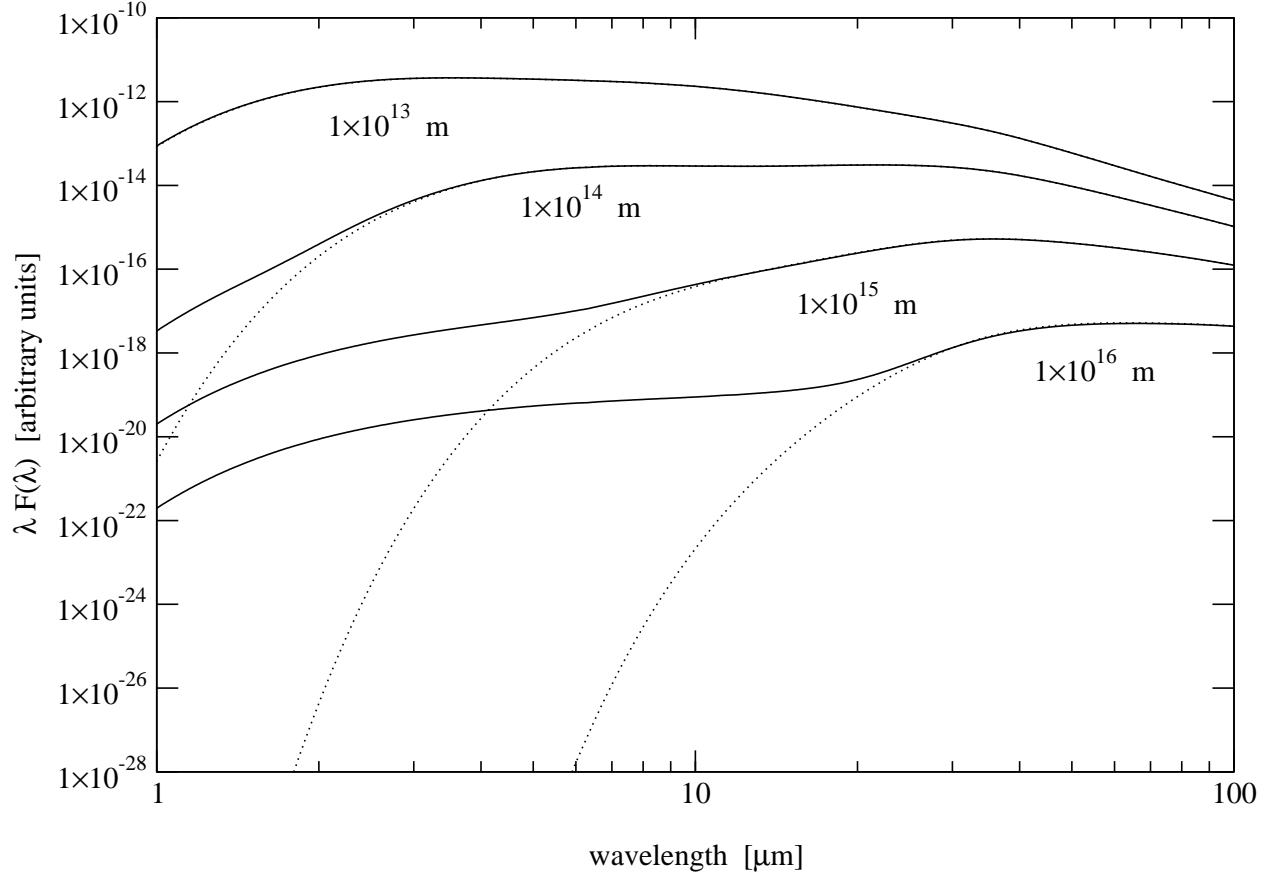


Fig. 2.— The emission of a thin, pure dust shell with temperature fluctuations (solid line) and the emission from equilibrium calculations (dotted line) at various distances to the central star. Illumination and dust parameters of the model are described in Table 2. Note the deviations between the two methods.

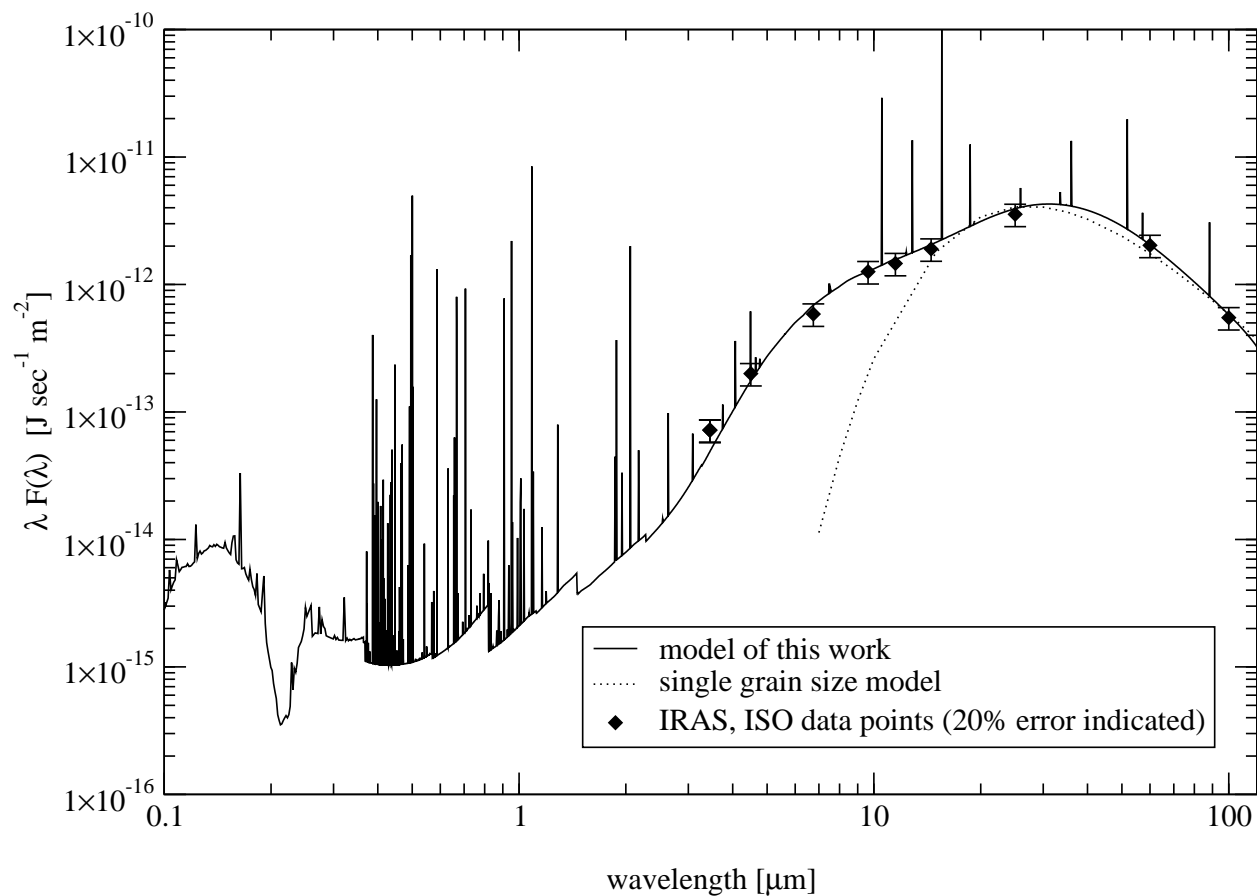


Fig. 3.— The model for V605 Aql using the emission from fluctuating dust grains. It has been calculated with the parameters given in Table 2. Diamonds represent the observations (Table 1) with 20 percent error bars. The dotted line is the single grain size model after Pollacco et al. (1992). Emission lines and absorption bands are due to the gaseous component in our model.

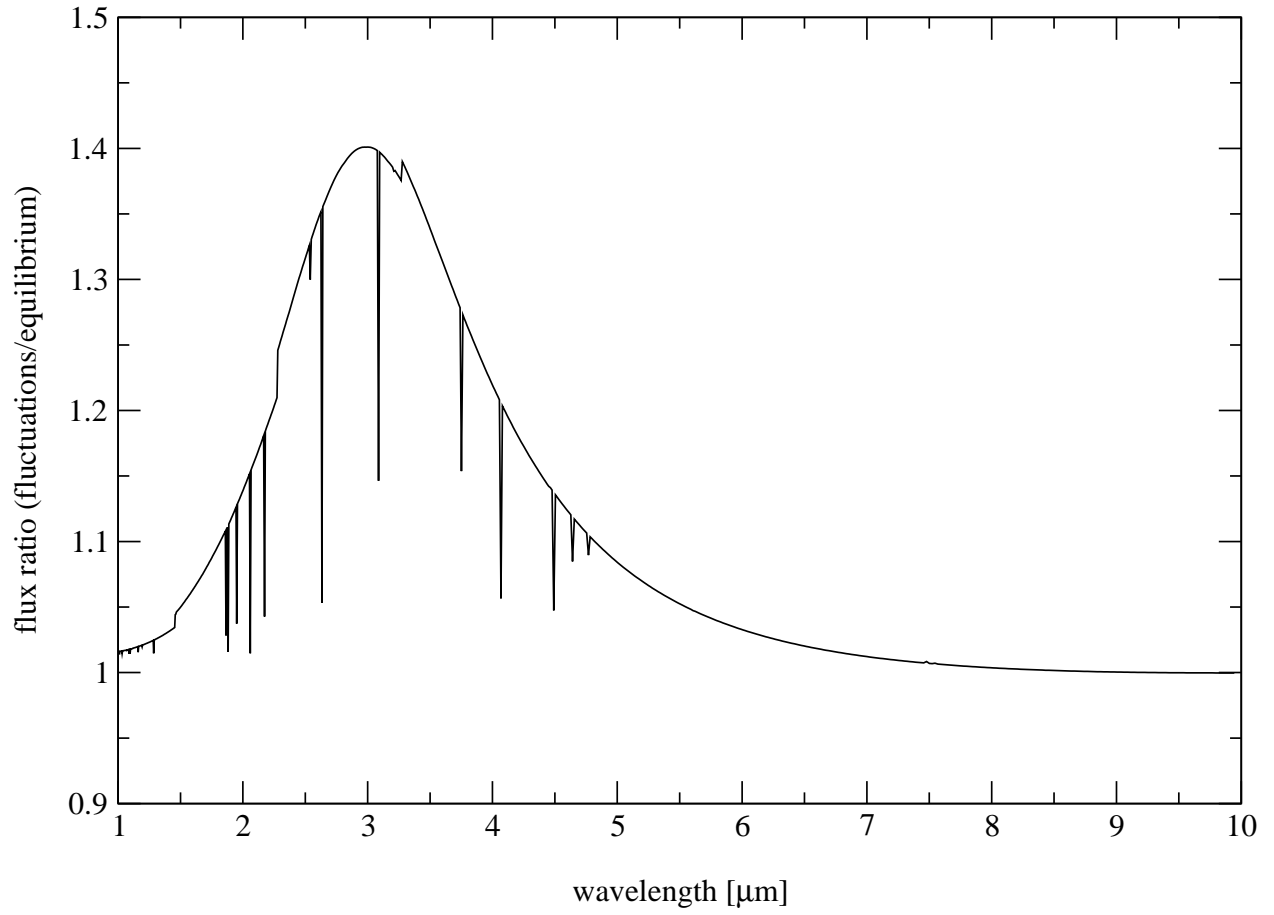


Fig. 4.— The ratio of the model using temperature fluctuations compared to using the emission by grains in equilibrium as a function of wavelength.

Table 1. IR Measurements Used in Modeling

Instrument	λ [μm]	F_ν [Jy]	λF_λ [W m^{-2}]
L ^a	3.45	0.083	7.21×10^{-14}
ISO LW1	4.50	0.3	2.00×10^{-13}
ISO LW5	6.75	1.3	5.87×10^{-13}
ISO LW7	9.63	4.1	1.26×10^{-12}
ISO LW8	11.50	5.6	1.46×10^{-12}
ISO LW9	14.5	9.2	1.90×10^{-12}
IRAS LW7	25	29.5	3.54×10^{-12}
IRAS LW10	60	40.6	2.03×10^{-12}
IRAS LW13	100	18.3	5.49×10^{-13}

^aThe L band value has been taken from van der Veen, Habing, & Geballe (1989)

Table 2. Model Parameters for V605 Aql

Parameter	Value
Gas shell	
Total gas mass	$7.6 \times 10^{-2} M_{\odot}$
Hydrogen abundance	H/He $\approx 10^{-6}$ solar
Heavy Elements	He/Y solar
Dust shell	
Inner radius	$r_{in} = 2.5 \times 10^{14}$ m
Outer radius	$r_{out} = 3.0 \times 10^{14}$ m
Total dust mass	$8.0 \times 10^{-3} M_{\odot}$
Visual extinction	$A_V = 7$ mag
Dust material	
Carbonaceous grains	
Grain size distribution (MRN)	$a_{min} = 6 \text{ \AA}, a_{max} = 4.55 \text{ \mu m}, p = 3.1$
Central star	
Luminosity	$L = 5800 L_{\odot}$
Temperature	$T = 100,000$ K black body
Adopted distance to Abell 58	$d = 5$ kpc